Excitation of Delocalized Long-Lived States ~~in~~of Aliphatic Protons at Low and High Magnetic Fields

Sebastiaan Van Dyck, Coline Wiame, Kirill F. Sheberstov* and Geoffrey Bodenhausen

Chimie Physique et Chimie du Vivant (CPCV, UMR 8228), Département de Chimie,

École Normale Supérieure, PSL University, Sorbonne Université,

75005 Paris, France

*Corresponding Author:

Dr Kirill Sheberstov email: kirill.sheberstov@ens.psl.eu

To be submitted to Magn. Reson. (Groupement Ampere)

SVD's ORCID: 0009-0005-7622-5753

KS's ORCID: 0000-0002-3520-6258

GB's ORCID: 0000-0001-8633-6098

CW ORCID: 0009-0008-3517-3354

Abstract

Long-lived states (LLS) can be excited in geminal protons of aliphatic chains by mono- or poly-chromatic spin-lock induced crossings (SLIC), i.e., by application of one or more selective radio-frequency (RF) fields to create delocalised population imbalances between states belonging to different symmetry under spin permutations. At low fields (in this work at 1.4 T, or 60 MHz for proton NMR), these experiments are challenging due to the proximity of the chemical shifts and the need to consider the full untruncated *J*-coupling Hamiltonian. Five molecules were studied in this work: ethanolamine, lysine, vitamin B1, metronidazole, and phenoxyethylamine (POEA). For POEA and metronidazole, the LLS are reported for the first time. Measurements were carried out at low and high magnetic fields (1.4 T and 11.7 T, or 60 and 500 MHz for protons) using 60 MHz Magritek and 500 MHz Bruker NEO spectrometers. The rates $R_{LLS} = 1/T_{LLS}$ and $R_1 = 1/T_1$ were determined using monochromatic SLIC excitation at both fields. We describe strategies for optimising SLIC conditions in cases where the signals of neighbouring CH_2 groups are relatively close to each other.

Key words

Long-lived states; Field-dependent relaxation; Spin-lock induced crossings.

Introduction

A long-lived state (LLS) is a nuclear spin state that has a lifetime longer than the longitudinal relaxation time [Carravetta et al., 2004]. Usually, an LLS corresponds to an imbalance between states with different spin permutation symmetries [Stevanato et al., 2015, Sheberstov et al., 2019a, Sabba et al. 2022]. In an isolated two-spin system with two protons H_A and $H_{A'}$, such an imbalance can occur between the average population of three symmetric triplet states ($|T_1\rangle$, $|T_0\rangle, |T_{-1}\rangle$) and the population of the singlet state ($|S_0\rangle$), which is antisymmetric under spin permutation. The resulting population imbalance is immune to relaxation due to the dipole-dipole coupling between the two protons H_A and $H_{A'}$, thus resulting in a long-lived state. In short *achiral* aliphatic chains -(CH_2-CH_2)- with 4 protons, the geminal proton pairs are chemically equivalent because of the lack of stereogenic centers, but they can be magnetically inequivalent provided each CH_2 group has a distinct chemical shift and provided the vicinal scalar couplings between neighbouring CH_2 groups differ. This occurs if the populations of the rotamers that result from rotations about the C-C bond are *not* equal, so that the differences between the vicinal couplings $\Delta J = J_{AX} - J_{AX'} = J_{A'X} - J_{A'X'}$ do not vanish. Magnetic inequivalence allows one to excite an LLS that is *delocalized* across the two AA' and XX' spin pairs. This can be achieved by mono- or poly-chromatic spin-lock induced crossings (SLIC) [DeVience et al., 2013, Sonnefeld et al., 2022a, Sonnefeld et al., 2022b], i.e., by application of one or two selective radio-frequency (RF) fields simultaneously. Although long-lived state excitation can alternatively, also be achieved via Adiabatic-Passage Spin Order Conversion (APSOC, [Pravdivtsev et al., 2016]), this work focuses exclusively on SLIC-based excitation methods. This paper focuses on mono-chromatic SLIC excitation solely. At high fields (e.g. 500 MHz), the RF amplitude for single quantum (SQ) conditions, must be $\nu_{SLIC}^{SQ} = 2J_{intra}$, where J_{intra} is an averaged value of the intrapair ~~coupling~~couplings between ~~the~~ geminal protons, e.g. $J_{intra} = \frac{1}{2}\{{}^2J(H_A, H_{A'}) + {}^2J(H_X, H_{X'})\}$. A pulse duration $\tau_{SLIC}^{SQ} = 1/(|\sqrt{2}\Delta J|)$ suffices for SQ level-anti-crossing (LAC). After a variable relaxation delay τ_{rel}, one applies a T_{00} filter which removes all terms other than the desired population imbalance [Tayler et al., 2020]. A second SLIC pulse then reconverts the LLS into observable magnetisation (Fig. 1).

Achiral aliphatic chains with suitable 4-spin systems are found in ethanolamine, lysine, vitamin B1, metronidazole, and phenoxyethylamine (POEA) (Fig. 2). At high field (e.g., at 11.7 T or 500 MHz for protons), all aliphatic chains in Fig. 2 can be described as AA'XX' systems in Pople's notation. On the other hand, at low field (e.g., at 1.4 T or 60 MHz) these systems must

be described by AA'BB' to account for the second-order couplings. We show that LLS in these molecules can be excited efficiently at 1.4 T, despite the strong coupling regime, using re-optimized SLIC sequences.

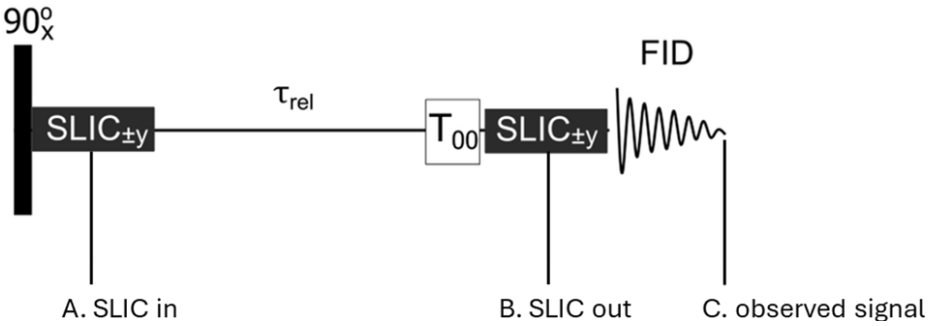

Figure 1. Sequence for the measurement of the relaxation times T_{LLS} of long-lived states (LLS) of protons in aliphatic chains comprising AA'XX' or AA'BB' systems. The π/2 pulse brings the magnetisation into the transverse plane. The first Spin-Lock Induced Crossing (SLIC) pulse converts this magnetisation into an LLS. This pulse is followed by a variable delay and a T_{00} filter that retains only singlet order, while the second SLIC pulse reconverts the LLS into observable magnetisation. Cycling of the RF phases along the ±y axes eliminates undesirable signals [Kiryutin et al., 2016]. In AA'XX' or AA'BB' systems, the SLIC pulses must be applied on resonance with either AA' or XX' spins.

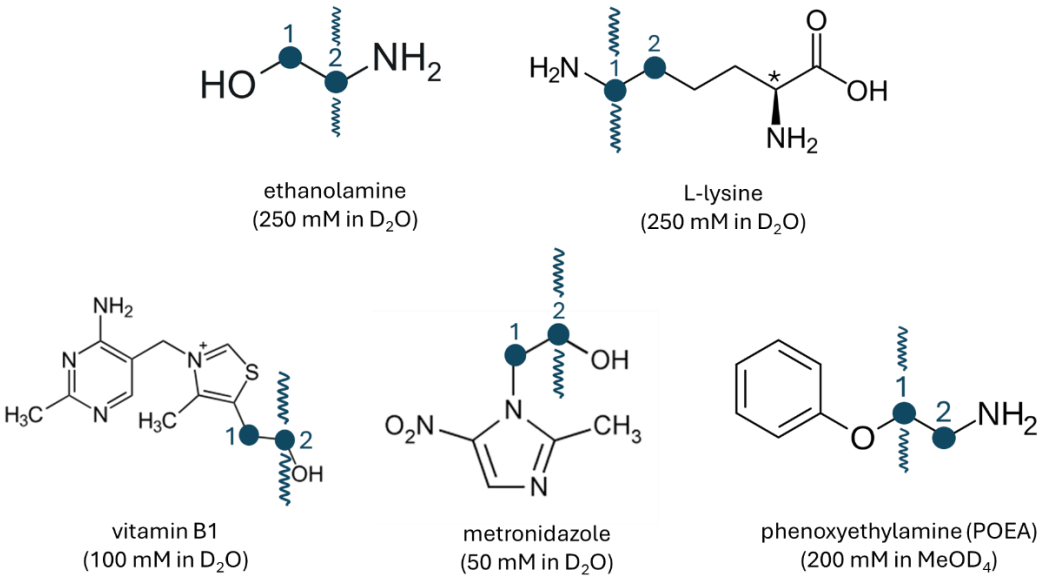

Figure 2. ~~Six~~Five molecules where long-lived states have been excited efficiently at both low and high static fields of 1.4 and 11.7 T (60 and 500 MHz for protons). All molecules shown are achiral and feature chemically equivalent but *magnetically inequivalent* proton pairs AA'XX' at high field and AA'BB' at low field. The wavy arrows indicate the CH_2 groups that were irradiated, in these experiments, to excite the LLS by mono-chromatic SLIC (arrows above the molecules), and to reconvert the LLS into magnetisation (arrows below the molecules). Note that one can also reconvert LLS on the adjacent CH2 group. The relaxation rates $R_1 = 1/T_1$ of the CH_2 groups were also determined by the conventional inversion-recovery method. All ligands were dissolved in D_2O at concentrations in the range between 50 and 250 mM, except for POEA which was dissolved in $MeOD_4$. These samples were not buffered. The reported pH values are 11.70 for ethanolamine, 6.00 for L-lysine, 2.70 for vitamin B1, 7.15 for metronidazole and 10.65 for POEA.

Methods

Strong Coupling at low field

As previously reported [Sonnefeld et al., 2022a, Sonnefeld et al., 2022b], the Hamiltonian of a 4-spin AA'XX' system at high magnetic fields (in this work at 11.7 T) only features strong couplings between the geminal pairs (e.g., H_A couples strongly to $H_{A'}$), but not between the vicinal protons (~~since~~ H_A couples weakly to H_X). ~~At low field however,~~Strong coupling is defined by $\Delta\delta < J$, whereas weak coupling holds when $\Delta\delta \gg J$. For a 4-spin system, $\Delta\delta$ is defined by the ~~vicinal~~ difference in chemical shift between the two adjacent CH_2 spin pairs (so AA' and XX'). The J-couplings are ~~also strong. The~~ constant. However, $\Delta\delta$ scales with the magnetic field; therefore, as we move to a lower magnetic field, $\Delta\delta$ decreases, which results in a higher ratio of J with respect to $\Delta\delta$. Therefore, the couplings between geminal proton spin pairs become stronger. That is why the Hamiltonian ~~can~~, at low magnetic field (i.e., 1.4 T), may be represented by ~~a~~the topological diagram ~~(Fig.~~shown in Figure 3~~)~~, where the geminal ~~J~~ couplings $J_{AA'}$ and $J_{BB'}$ are approximately equal, while the vicinal couplings are pairwise degenerate $J_{AB} = J_{A'B'}$ and $J_{A'B} = J_{AB'}$.

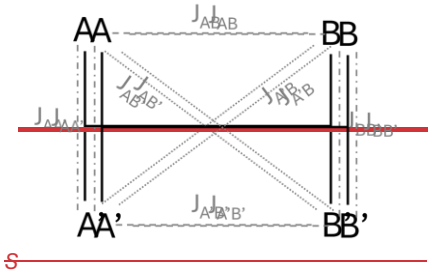

Figure 3. Topological representation of a 4 spin AA'BB' system

The Hamiltonian in units of Hz is:

$$H = \nu_{AA'}(\hat{I}_{Az} + \hat{I}_{Az'}) + \nu_{BB'}(\hat{I}_{Bz} + \hat{I}_{Bz'}) + J_{AA'}\hat{\boldsymbol{I}}_A \cdot \hat{\boldsymbol{I}}_{A'} + J_{BB'}\hat{\boldsymbol{I}}_B \cdot \hat{\boldsymbol{I}}_{B'}$$
$$+J_{AB}\hat{\boldsymbol{I}}_A \cdot \hat{\boldsymbol{I}}_B + J_{AB'}\hat{\boldsymbol{I}}_A \cdot \hat{\boldsymbol{I}}_{B'} + J_{A'B}\hat{\boldsymbol{I}}_{A'} \cdot \hat{\boldsymbol{I}}_B + J_{A'B'}\hat{\boldsymbol{I}}_{A'} \cdot \hat{\boldsymbol{I}}_{B'} \quad (1)$$

Where $\hat{\boldsymbol{I}}_i$ corresponds to vector representation of spin operator of spin i, operators $\hat{I}_{iz}$ represent z component of the operator $\hat{\boldsymbol{I}}_i$. When switching from strong coupling at low field to weak coupling at high field, the non-secular terms of the vicinal *J* couplings (but not those due to the geminal couplings) can be dropped:

$$H_{vic}^{LF} = J_{AB}\hat{\boldsymbol{I}}_A \cdot \hat{\boldsymbol{I}}_B + J_{AB'}\hat{\boldsymbol{I}}_A \cdot \hat{\boldsymbol{I}}_{B'} + J_{A'B}\hat{\boldsymbol{I}}_{A'} \cdot \hat{\boldsymbol{I}}_B + J_{A'B'}\hat{\boldsymbol{I}}_{A'} \cdot \hat{\boldsymbol{I}}_{B'}$$

$$H_{vic}^{HF} = J_{AB}\hat{I}_{Az}\hat{I}_{Bz} + J_{AB'}\hat{I}_{Az}\hat{I}_{Bz'} + J_{A'B}\hat{I}_{Az'}\hat{I}_{Bz} + J_{A'B'}\hat{I}_{Az'}\hat{I}_{Bz'} \quad (2)$$

Effects of second-order vicinal couplings

In a low static field, a weak RF field applied to H_A and $H_{A'}$ also affects the protons H_B and $H_{B'}$ ~~by a Bloch-Siegert shift that modifies the effective resonance frequency of the non-irradiated spins. However, this does not have any dramatic consequences for mono-chromatic SLIC.~~. At high field, these effects are negligible, so that monochromatic SLIC is truly selective. At low magnetic fields, we have investigated the effects of second-order couplings, for mono-chromatic SLIC excitation, using simulations with Spin Dynamica [Bengs et al., 2018] written using the Wolfram Mathematica software package.

In a 4-spin system AA'BB', the LLS part of the density operator $\hat{\sigma}_{LLS}$, i.e., the population imbalances, always comprises three terms, regardless of how one excites the LLS [Sonnefeld et al., 2022a]:

$$\hat{\sigma}_{LLS} = \lambda_{LLS}\left(-\frac{1}{3}\hat{\boldsymbol{I}}_A \cdot \hat{\boldsymbol{I}}_{A'} - \frac{1}{3}\hat{\boldsymbol{I}}_B \cdot \hat{\boldsymbol{I}}_{B'} + \frac{8}{9}\left(\hat{\boldsymbol{I}}_A \cdot \hat{\boldsymbol{I}}_{A'}\right)\left(\hat{\boldsymbol{I}}_B \cdot \hat{\boldsymbol{I}}_{B'}\right)\right). \quad (3)$$

The LLS yields have been simulated for mono-chromatic SLIC irradiation applied to AA'. We chose typical values for a 4-spin system: $J_{AA'} = J_{BB'} = -14$ Hz, $J_{AB} = J_{A'B'} = 5$ Hz and $J_{A'B} = J_{AB'} = 9$ Hz, hence $\Delta J = -4$ Hz. At high fields, where the secular approximation can be invoked, the optimum RF amplitude for the single-quantum (SQ-LAC) condition is $\nu_{SLIC} = 2J_{intra} = -28$ Hz, and the optimum SLIC duration is $\tau_{SLIC} = 1/(\Delta J\sqrt{2}) = 177$ ms [Sonnefeld et al., 2022b].

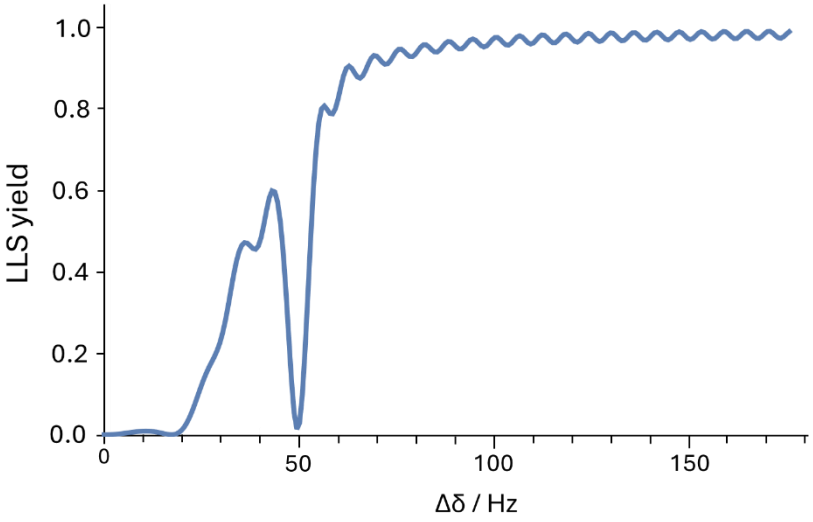

Figure 4. Simulated yields of the excitation of a long-lived state (LLS) as defined in Eq. (3) as a function of the chemical shift difference (Δδ) between the AA′ and BB′ spin pairs in a 4-spin system. Parameters of SLIC pulse were ν_{SLIC} = 28 Hz and τ_{SLIC} = 177 ms corresponding to the high-field SLIC conditions. LLS yield is normalized to 1 with respect to the high-field regime, which is achieved at the plateau on the right-hand side of the figure.

Fig. 4 also shows how the LLS yield depends on the chemical shift difference between spins ~~A~~pairs AA' and ~~X denoted as~~ BB'. The simulations were done for the case of high-field SLIC conditions (ν_{SLIC} = 28 Hz, τ_{SLIC} = 177 ms). At Δδ > 60 Hz the LLS yield reaches a plateau that we normalized to 1. The sudden drop in LLS yield, here at 50 Hz, depends on J_{intra}; for higher values of J_{intra}, the dip shifts to higher frequencies. This means there is a "blind spot" where excitation of LLS cannot be achieved, at least not starting with high-field SLIC parameters. The blind spot can be understood from the dynamics of the off-resonant BB' spins in the rotating frame. Although these spins are not meant to be directly addressed by the SLIC irradiation applied to the AA'pair, they experience an effective field of magnitude $\nu_1^{eff} = \sqrt{\Delta\delta^2 + \nu_{SLIC}^2}$, where $\Delta\delta$ is the frequency offset between the two spin pairs. The dip in the LLS efficiency occurs when this effective nutation frequency matches $2\nu_{SLIC}$, which gives the condition $\Delta\delta = \sqrt{3}\,\nu_{SLIC}$.

In ~~Fig.~~Figure 4, under high-field SLIC conditions (ν_{SLIC} = 28 Hz, τ_{SLIC} = 177 ms), the LLS yield is 1.0 for 250 Hz and drops down to 0.35 for Δδ = 52 Hz. ~~Fig.~~Figure 4 ~~also~~ shows how the LLS yield depends on the chemical shift difference.

The simulations of Fig. 5 show how to optimize the RF amplitude ν_{SLIC} and the SLIC duration τ_{SLIC}, for the strong coupling regime and single quantum conditions, to achieve the best LLS

yields at different values for Δδ = 250 Hz (high-field regime) and Δδ = 52 Hz (low-field regime). The figure shows the LLS conversion efficiency normalized to 1 with respect to the high-field regime, which is achieved at the plateau on the right-hand side of the figure. Maximum conversion efficiency in the aliphatic spin networks for 4 spin systems for monochromatic SLIC applied to AA' spins is achieved when a full population of the $T_{+1}^{AA'}T_{0}^{BB'}$ or $T_{-1}^{AA'}T_{0}^{BB'}$ state is transferred to $S_{0}^{AA'}S_{0}^{BB'}$ state. This corresponds to ±5/72 ≈ 7% population imbalance between the 9 triplet-triplet states and a unique singlet-singlet state.

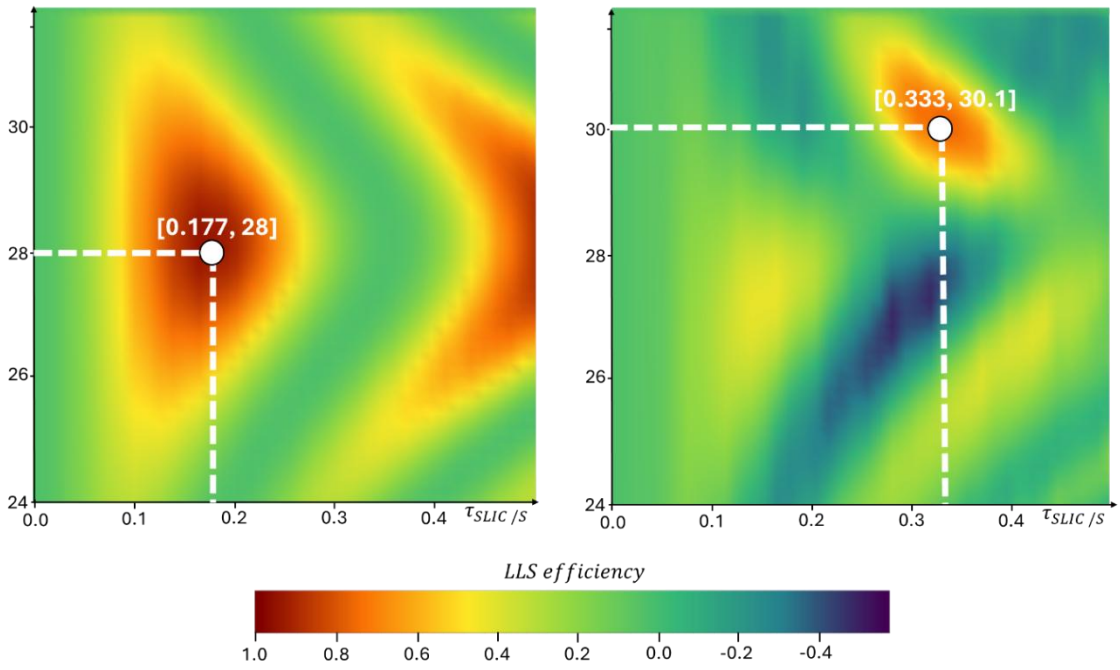

Figure 5. Left panel shows that for a large difference $\Delta\delta$ = 250 Hz, the single-quantum SLIC condition (RF amplitude ν_{SLIC} in the vertical dimension and the duration τ_{SLIC} in the horizontal dimension) for a 4-spin system (ν_{SLIC} = 28 Hz, τ_{SLIC} = 177 ms) match the theoretical conditions at high-field ($\nu_{SLIC} = 2J_{intra}$, $\tau_{SLIC} = 1/(\Delta J\sqrt{2})$). However, when the difference is small ($\Delta\delta$ = 52 Hz), the optimum SLIC conditions are ν_{SLIC} = 30.1 Hz while τ_{SLIC} = 333 ms. The change in ν_{SLIC} is subtle (+ 7 %), but the SLIC duration changes drastically (+ 83 %). Since aliphatic -CH_2- groups in many of the selected molecules (Fig. 2) have $\Delta\delta$ < 60 Hz at 1.4 T, their SLIC duration τ_{SLIC} and SLIC amplitude ν_{SLIC} must be re-optimised. LLS efficiency is normalized to 1 with respect to the high-field regime, which is achieved at the maximum on the left panel.

According to ~~Fig.~~Figure 5, the LLS yield after re-optimisation of ν_{SLIC} and τ_{SLIC}, is 0.8 for $\Delta\delta$ = 52 Hz. We can compare it with the LLS yield in ~~Fig.~~Figure 4 (~ 0.35) to obtain the enhancement factor. The ratio of the optimised LLS yield/non-optimised LLS yield is equal to: 0.8/0.35 ≈ 2.3.

Subsequently, we re-optimised τ_{SLIC} and ν_{SLIC} for each molecule experimentally. The SLIC conditions at 11.7 and 1.4 T are displayed in Table 1, whereas Table 2, shows the improvement in the experimentally achieved LLS yield upon re-optimisation of τ_{SLIC} and ν_{SLIC} at 1.4 T.

Table 1. Experimentally optimised SLIC conditions for 4-spin systems at low (1.4 T) and high (11.7 T) fields. The SLIC amplitude ν_{SLIC} changes for vitamin B1 and metronidazole~~,~~ but remains unchanged for the other ligands. The duration τ_{SLIC} increases at low magnetic field for ethanolamine, vitamin B1 and metronidazole. Note that the reported SLIC conditions for ethanolamine and vitamin B1 deviate from previously reported values (Sonnefeld et al., 2022a), as the molecules for the presented result in this work were not prepared in buffer. Shifts in pH values can affect SLIC conditions, particularly for ethanolamine. The reported pH values for molecules prepared in D_2O are: 11.70 for ethanolamine, 6.00 for lysine, 2.70 for vitamin B1 and 7.15 for metronidazole.

Molecule	~~Δν (~~Δδ (Hz) at 1.4 T (60 MHz)	ν_{SLIC} (Hz) at 11.7 T (500 MHz)	ν_{SLIC} (Hz) at 1.4 T (60 MHz)	τ_{SLIC} (ms) at 11.7 T (500 MHz)	τ_{SLIC} (ms) at 1.4 T (60 MHz)
ethanolamine	54	~~25~~24	25	~~190~~350	~~340~~380
lysine	80	27	27	205	205
vitamin B1	42	26	27	~~250~~240	320
metronidazole	36	26	27	250	310
POEA	61	23	23	240	240

Table 2. LLS yield at 1.4 T before re-optimisation of ν_{SLIC} and τ_{SLIC} (using the conditions listed in columns 3 and 5 in Table 1) and after re-optimisation of ν_{SLIC} and τ_{SLIC} (using the conditions listed in column 4 and 6 in Table 1). The LLS yield with respect to the thermal signal (when the number of transients and the receiver gain remain the same) is lower than at conventional high-field, where the yield is approximately ~ 10% (Sonnefeld et al., 2022a). However, the third column shows that an enhancement, up to a factor of 3.6, has been achieved. This illustrates the need for re-optimisation of ν_{SLIC} and τ_{SLIC} when $\Delta\delta < 60\ Hz$ at low magnetic fields. For lysine and POEA for which the difference in chemical shifts $\Delta\delta > 60\ Hz$~~-~~, the SLIC conditions were identical at 11.7 T and 1.4 T, so no increase in yield was observed.

Molecule	LLS Yield (with respect to thermal) (Non-optimised SLIC) / %	LLS Yield (with respect to thermal) (Optimised SLIC) / %	Enhancement Factor (Optimised/Non-optimised)
ethanolamine	~~0~~5.68	~~2.06~~6.25	~~3.0~~1.1
lysine	~~1.89~~2.55	~~1.89~~2.55	1.0
vitamin B1	~~1.25~~2.12	~~2.11~~3.50	1.7
metronidazole	~~0.78~~1.11	~~2.21~~4.06	~~2.8~~3.6
POEA	~~4.69~~6.25	~~4.69~~6.25	1.0

Comparing T_{LLS} and T_1 relaxation time constants at different magnetic fields

The T_1 and T_{LLS} of all five molecules shown in Fig. 2 were measured at low and high static fields, in the same sample tubes, at the same concentrations, in the same solvents and at the same temperatures. The concentrations were chosen to be high to warrant sufficient sensitivity at low field, bearing in mind that the efficiency of two-way ("in-and-out") SLIC is on the order of only 10%. In the future we aim to enhance the sensitivity by combining SLIC at both low and high fields with Dynamic Nuclear Polarisation [Vasos et al., 2009, Tayler et al., 2012, Bornet et al., 2014, Kiryutin et al., 2019a, Kiryutin et al., 2019b, Razanahoera et al., 2024.]

The ratios of the relaxation rates of long-lived states ($R_{LLS} = 1/T_{LLS}$) and of longitudinal magnetisation ($R_1 = 1/T_1$), are different at low and high fields (60 and 500 MHz for protons). The ratio T_{LLS}/T_1 provides a measure of the usefulness of LLS for various applications such as the measurement of slow motions [Sarkar et al., 2007], or small translation diffusion coefficients [Cavadini et al., 2005].

Results and discussion

Inversion-recovery experiments at both low and high fields provided T_1 values for all samples. The signal integrals of a chosen multiplet (see wavy arrows in Fig. 2) were plotted as a function of the relaxation delay τ_{rel}. ~~Fig.~~Figure 6 shows the results obtained at low field. The same T_1 experiments were repeated at high magnetic field (11.7 T). The results are summarised in Table 3.

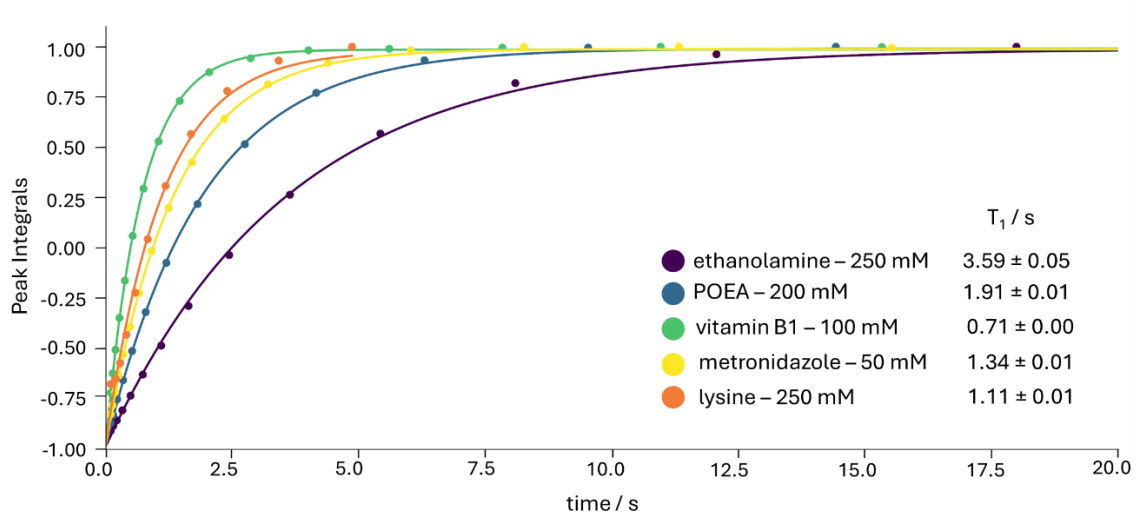

Figure 6. Longitudinal T_1 relaxation at low field (1.4 T) of the CH_2 protons highlighted by curly arrows in the 5 molecules shown in Fig. 2, measured by inversion recovery.

To determine the lifetimes T_{LLS} at low field (1.4 T) by SLIC experiments, the delay τ_{rel} in Fig. 1 was incremented for each of the 5 molecules shown in Fig. 2.

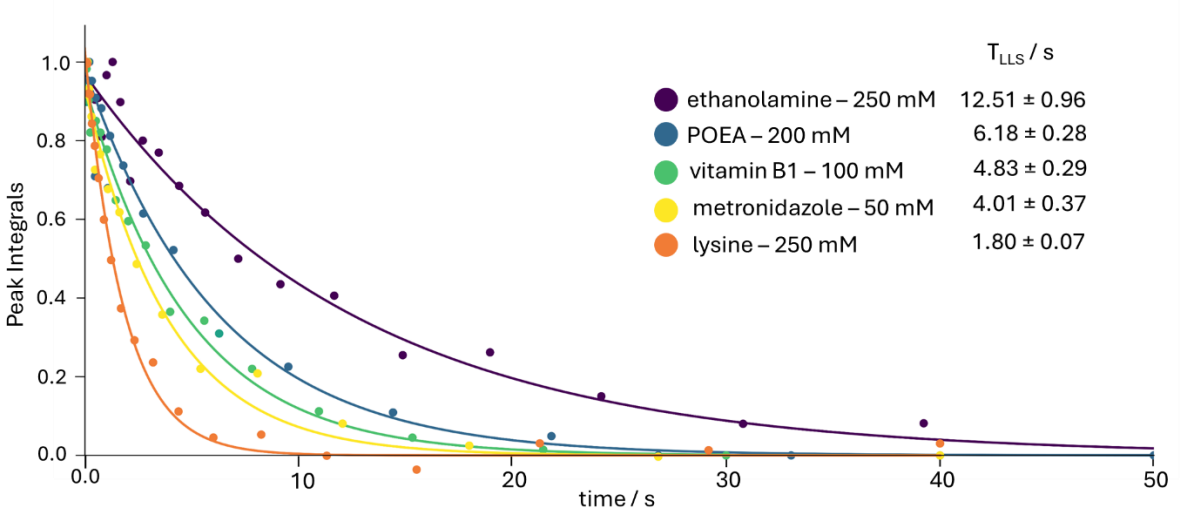

Figure 7. LLS decays at low field (1.4 T) of the aliphatic CH_2 protons highlighted by curly arrows in the 5 molecules drawn ~~Fig.~~ Figure 2.

Again, these experiments were also carried out with the same samples at high field. The high and low field results are shown in Tables 3 and 4. The effect of the magnetic field on the ratio T_{LLS}/T_1 is shown in Table 5.

Table 3. T_1 and T_{LLS} values at high field (11.7 T)

Molecule	Concentration (mM)	CH_2 group (see Fig. 2)	T_1^{HF} /s (500 MHz)	T_{LLS}^{HF} /s (500 MHz)
ethanolamine	250	2	3.46 ± 0.01	10.33 ± 1.88

lysine	250	1	1.40 ± 0.01	4.33 ± 0.08
vitamin B1	100	2	0.73 ± 0.01	5.58 ± 0.27
metronidazole	50	2	1.27 ± 0.02	3.81 ± 0.14
POEA	200	1	2.21 ± 0.02	9.21 ± 0.49

Table 4. T_1 and T_{LLS} values at low field (1.4 T or 60 MHz for protons)

Molecule	Concentration (mM)	CH_2 group (see Fig. 2)	T_1^{LF} LF/s (60 MHz)	T_{LLS}^{LF} /s (60 MHz)
ethanolamine	250	2	3.59 ± 0.05	12.51 ± 0.96
lysine	250	1	1.11 ± 0.01	1.80 ± 0.07
vitamin B1	100	2	0.71 ± 0.00	4.83 ± 0.29
metronidazole	50	2	1.34 ± 0.01	4.01 ± 0.37
POEA	200	1	1.91 ± 0.01	6.18 ± 0.28

Table 5. Ratios T_{LLS} / T_1 at high field (11.7 T) and at low field (1.4 T).

Molecule in D_2O	Concentration (mM)	enhancement $(T_{LLS}/T_1)^{HF}$ (500 MHz)	enhancement $(T_{LLS}/T_1)^{LF}$ (60 MHz)	ratio of enhancements HF/LF
ethanolamine	250	3.0	3.5	0.86
lysine	250	3.1	1.6	1.94
vitamin B1	100	7.6	6.8	1.12
metronidazole	50	3.0	3.0	1.00
POEA	200	4.2	3.2	1.31

Comparison between the relaxation times T_{LLS} and T_1 at high field gives a range $3.0 < T_{LLS}/T_1 < 4.2$ for all molecules except vitamin B1, which has an exceptional gain $T_{LLS}/T_1 = 7.6$. At low field, by contrast, the ratios lie in the range of $3.0 < T_{LLS}/T_1 < 6.8$ for all molecules except lysine, which has a rather modest gain $T_{LLS}/T_1 = 1.6$. In summary, the T_{LLS}/T_1 ratios at high field (11.7 T) are either slightly higher or similar as at low field (1.4 T), except for ethanolamine where the enhancement is 17 % higher at low field.

Conclusions

The yield of the excitation of LLS by SLIC at low fields depends on the chemical shift difference Δδ between the neighbouring spin pairs. When $\Delta\delta \leq 60$ Hz, the pulse amplitude, ν_{SLIC}, and duration, τ_{SLIC}, must be optimised experimentally starting at the high-field conditions. The T_{LLS}/T_1 ratios at low field (1.4 T) are either slightly lower or similar as at high field.

Acknowledgments

We are grateful to the reviewers, Prof. Danila A. Barskiy and Dr. Mohammed Sabba, who helped us to improve the quality of the manuscript.

Data availability

The Spin Dynamica codes used to calculate Figures 4 and 5 are available through the Zenodo repository under 10.5281/zenodo.18684154

Author Contributions

K.S. designed the research. S.V.D. and C.W. performed the experiments and analysed the data. All authors contributed to writing the paper.

Conflict of Interest

G.B. is a member of the editorial board of Magnetic Resonance of the Groupement Ampere. The authors have no other competing interests to declare.

Financial Support

This work was supported by the European Research Council (ERC), Synergy grant "Highly Informative Drug Screening by Overcoming NMR Restrictions" (HISCORE, grant agreement number 951459). K.S. acknowledges support by l'Agence Nationale de la Recherche (ANR) on the project THROUGH-NMR (ANR-24-CE93-0011-01).

References

Bengs, C., & Levitt, M. H. (2018). SpinDynamica: Symbolic and numerical magnetic resonance in a Mathematica environment. Magnetic Resonance in Chemistry, 56(6), 374–414. https://doi.org/10.1002/mrc.4642

Bornet, A., Ji, X., Mammoli, D., Vuichoud, B., Milani, J., Bodenhausen, G., and Jannin, S.: Long-Lived States of Magnetically Equivalent Spins Populated by Dissolution-DNP and Revealed by Enzymatic Reactions, Chem. – Eur. J., 20, 17113–17118, https://doi.org/10.1002/chem.201404967, 2014.

Carravetta, M., & Levitt, M. H. (2004). Long-lived nuclear spin states in high-field solution NMR. Journal of the American Chemical Society, 126(20), 6228–6229. https://doi.org/10.1021/ja0490931

Cavadini, S., Dittmer, J., Antonijevic, S., and Bodenhausen, G.: Slow Diffusion by Singlet State NMR Spectroscopy, J. Am. Chem. Soc., 127, 15744–15748, https://doi.org/10.1021/ja052897b, 2005.

DeVience, S. J., Walsworth, R. L., and Rosen, M. S.: Preparation of Nuclear Spin Singlet States Using Spin-Lock Induced Crossing, Phys. Rev. Lett., 111, 173002, https://doi.org/10.1103/PhysRevLett.111.173002, 2013.

Kiryutin, A. S., Panov, M. S., Yurkovskaya, A. V., Ivanov, K. L., and Bodenhausen, G.: Proton Relaxometry of Long-Lived Spin Order, ChemPhysChem, 20, 766–772, https://doi.org/10.1002/cphc.201800960, 2019a.

Kiryutin, A. S., Pravdivtsev, A. N., Yurkovskaya, A. v., Vieth, H.-M., & Ivanov, K. L.:Nuclear Spin Singlet Order Selection by Adiabatically Ramped RF Fields. The Journal of Physical Chemistry B, 120(46), 11978–11986. https://doi.org/10.1021/acs.jpcb.6b08879, 2016.

Kiryutin, A. S., Rodin, B. A., Yurkovskaya, A. V., Ivanov, K. L., Kurzbach, D., Jannin, S., Guarin, D., Abergel, D., and Bodenhausen, G.: Transport of hyperpolarized samples in dissolution-DNP experiments, Phys. Chem. Chem. Phys., 21, 13696–13705, https://doi.org/10.1039/C9CP02600B, 2019b.

Pravdivtsev, A. N., Kiryutin, A. S., Yurkovskaya, A. V., Vieth, H.-M., Ivanov, K. L.: Robust conversion of singlet spin order in coupled spin-1/2 pairs by adiabatically ramped RF-fields, J. Magn. Reson., 273, 56-64, https://doi.org/10.1016/j.jmr.2016.10.003, 2016.

Razanahoera, A., Sonnefeld, A., Sheberstov, K., Narwal, P., Minaei, M., Kouřil, K., Bodenhausen, G., and Meier, B.: Hyperpolarization of Long-Lived States of Protons in Aliphatic Chains by Bullet Dynamic Nuclear Polarization, Revealed on the Fly by Spin-Lock-Induced Crossing, J. Phys. Chem. Lett., 15, 9024–9029, https://doi.org/10.1021/acs.jpclett.4c01457, 2024.

Sabba, M., Wili, N., Bengs, C., Whipham, J. W., Brown, L. J., and Levitt, M. H.: Symmetry-based singlet–triplet excitation in solution nuclear magnetic resonance, J. Chem. Phys., 157, 134302, https://doi.org/10.1063/5.0103122, 2022.

Sarkar, R., Vasos, P. R., and Bodenhausen, G.: Singlet-State Exchange NMR Spectroscopy for the Study of Very Slow Dynamic Processes, J. Am. Chem. Soc., 129, 328–334, https://doi.org/10.1021/ja0647396, 2007.

Sheberstov, K. F., Kiryutin, A. S., Bengs, C., Hill-Cousins, J. T., Brown, L. J., Brown, R. C. D., Pileio, G., Levitt, M. H., Yurkovskaya, A. V., and Ivanov, K. L.: Excitation of singlet–triplet coherences in pairs of nearly-equivalent spins, Phys. Chem. Chem. Phys., 21, 6087–6100, https://doi.org/10.1039/C9CP00451C, 2019a.

Sonnefeld, A., Razanahoera, A., Pelupessy, P., Bodenhausen, G., and Sheberstov, K.: Long-lived states of methylene protons in achiral molecules, Sci. Adv., 8, eade2113, https://doi.org/10.1126/sciadv.ade2113, 2022a.

Sonnefeld, A., Bodenhausen, G., and Sheberstov, K.: Polychromatic Excitation of Delocalized Long-Lived Proton Spin States in Aliphatic Chains, Phys. Rev. Lett., 129, 183203, https://doi.org/10.1103/PhysRevLett.129.183203, 2022b.

Stevanato, G., Hill-Cousins, J. T., Håkansson, P., Roy, S. S., Brown, L. J., Brown, R. C. D., Pileio, G., and Levitt, M. H.: A Nuclear Singlet Lifetime of More than One Hour in Room-Temperature Solution, Angew. Chem. Int. Ed., 54, 3740–3743, https://doi.org/10.1002/anie.201411978, 2015.

Tayler, M. C. D.: Filters for Long-lived Spin Order, https://doi.org/10.1039/9781788019972-00188, 2020.

Tayler, M. C. D., Marco-Rius, I., Kettunen, M. I., Brindle, K. M., Levitt, M. H., and Pileio, G.: Direct Enhancement of Nuclear Singlet Order by Dynamic Nuclear Polarization, J. Am. Chem. Soc., 134, 7668–7671, https://doi.org/10.1021/ja302814e, 2012.

Vasos, P. R., Comment, A., Sarkar, R., Ahuja, P., Jannin, S., Ansermet, J.-P., Konter, J. A., Hautle, P., van den Brandt, B., and Bodenhausen, G.: Long-lived states to sustain hyperpolarized magnetization, Proc. Natl. Acad. Sci., 106, 18469–18473, https://doi.org/10.1073/pnas.0908123106, 2009.